

## Supporting Information

### A novel Fe-free photo-electro-Fenton-like system for enhanced ciprofloxacin destruction: bifunctional Z-scheme $\text{WO}_3/\text{g-C}_3\text{N}_4$

Xiaoyu Bai<sup>a</sup>, Yi Li<sup>a\*</sup>, Liangbo Xie<sup>a</sup>, Xiaohui Liu<sup>a</sup>, Sihui Zhan<sup>b\*</sup>, Wenping Hu<sup>a</sup>

<sup>a</sup> Tianjin Key Laboratory of Molecular Optoelectronic Sciences, Department of Chemistry, School of Science, Tianjin University & Collaborative Innovation Center of Chemical Science and Engineering (Tianjin), Tianjin 300072, China.

<sup>b</sup> Key Laboratory of Pollution Processes and Environmental Criteria (Ministry of Education), College of Environmental Science and Engineering, Nankai University, Tianjin 300071, China.

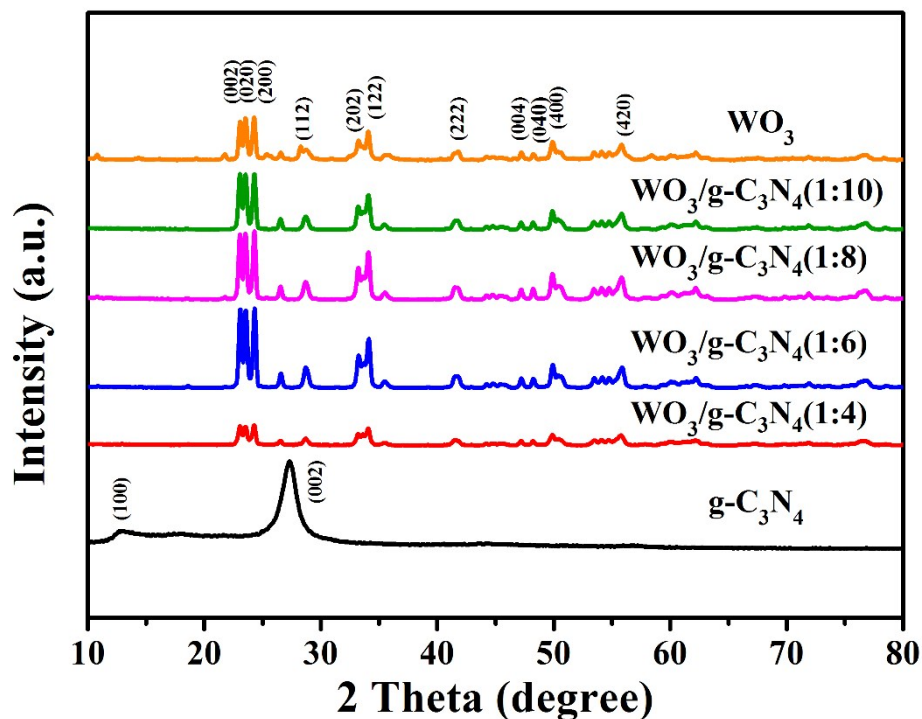


**Fig. S1** XRD patterns of  $\text{WO}_3/\text{g-C}_3\text{N}_4$ ,  $\text{WO}_3$  and  $\text{g-C}_3\text{N}_4$ .

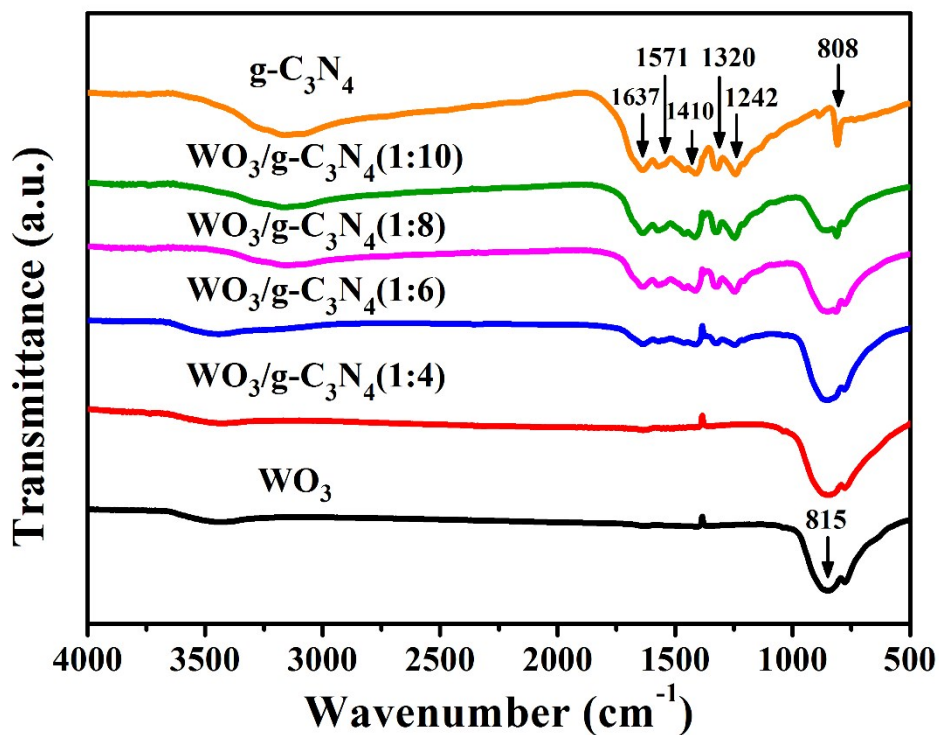


**Fig. S2** FT-IR spectrum of  $\text{WO}_3/\text{g-C}_3\text{N}_4$ ,  $\text{WO}_3$  and  $\text{g-C}_3\text{N}_4$ .

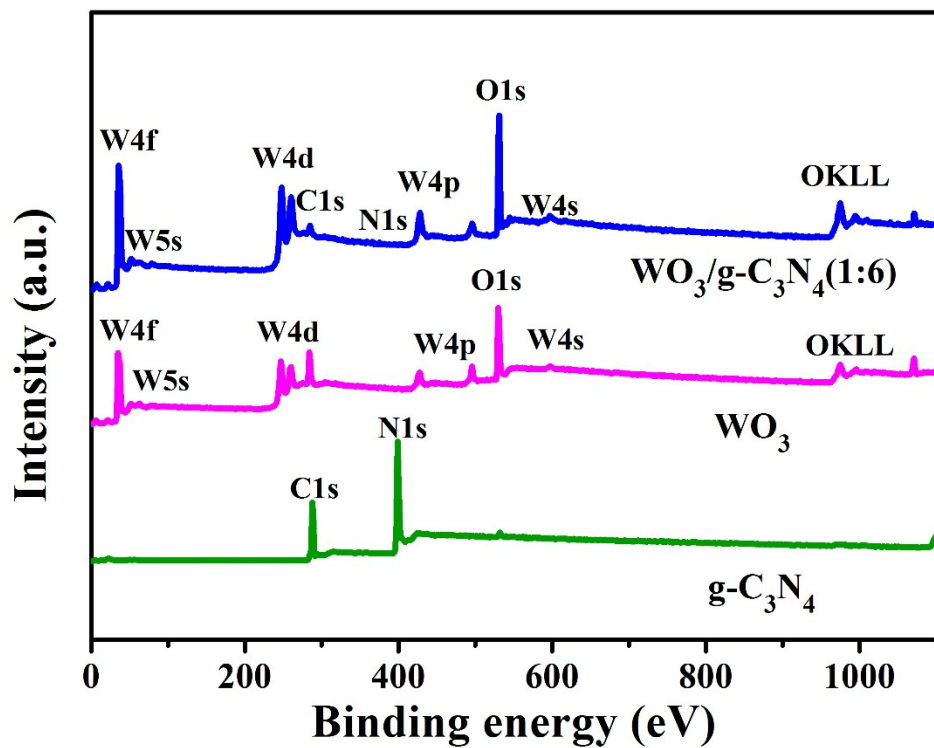


**Fig. S3** XPS survey of  $\text{WO}_3/\text{g-C}_3\text{N}_4(1:6)$ ,  $\text{WO}_3$  and  $\text{g-C}_3\text{N}_4$ .

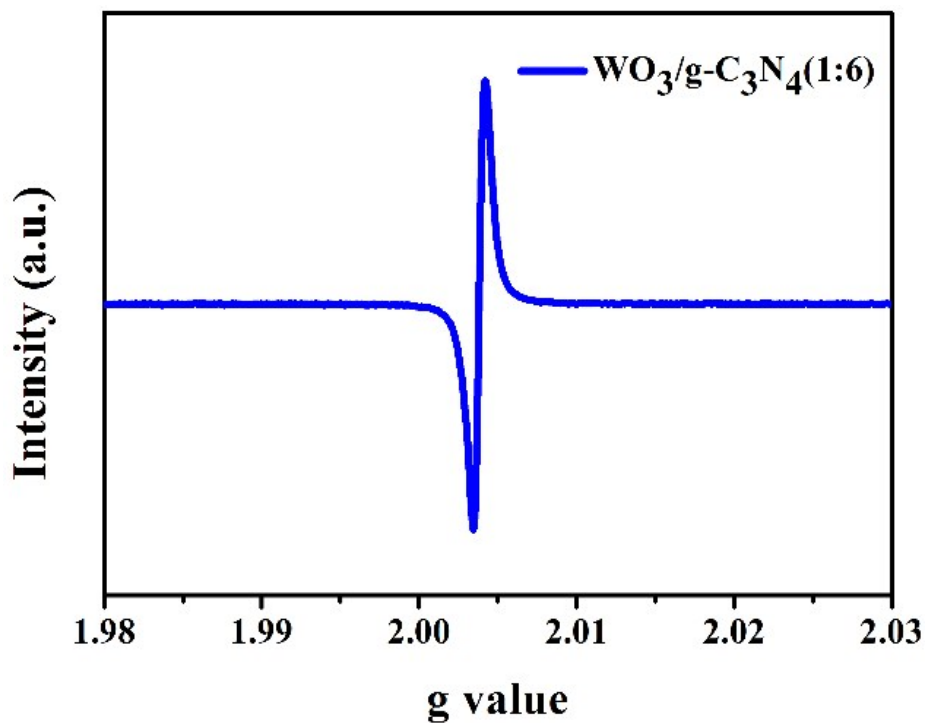


**Fig. S4** EPR spectrum of  $\text{WO}_3/\text{g-C}_3\text{N}_4(1:6)$ .

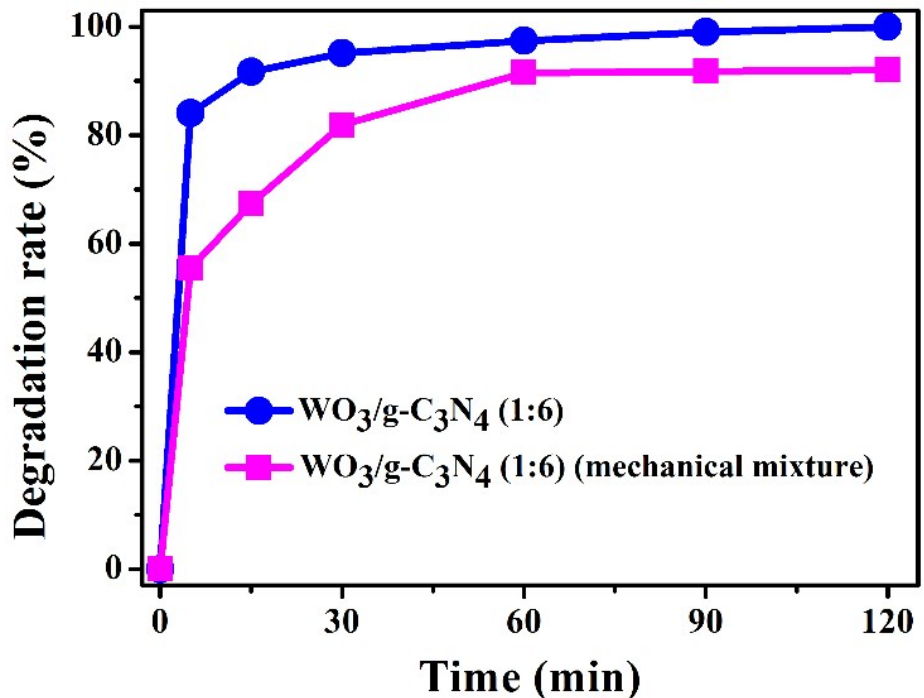


**Fig. S5** Degradation rate of CIP with  $\text{WO}_3/\text{g-C}_3\text{N}_4$  (1:6) and the mechanical mixture containing  $\text{WO}_3$  and  $\text{g-C}_3\text{N}_4$  with molar ratio 1:6 in PEF-like system, respectively.

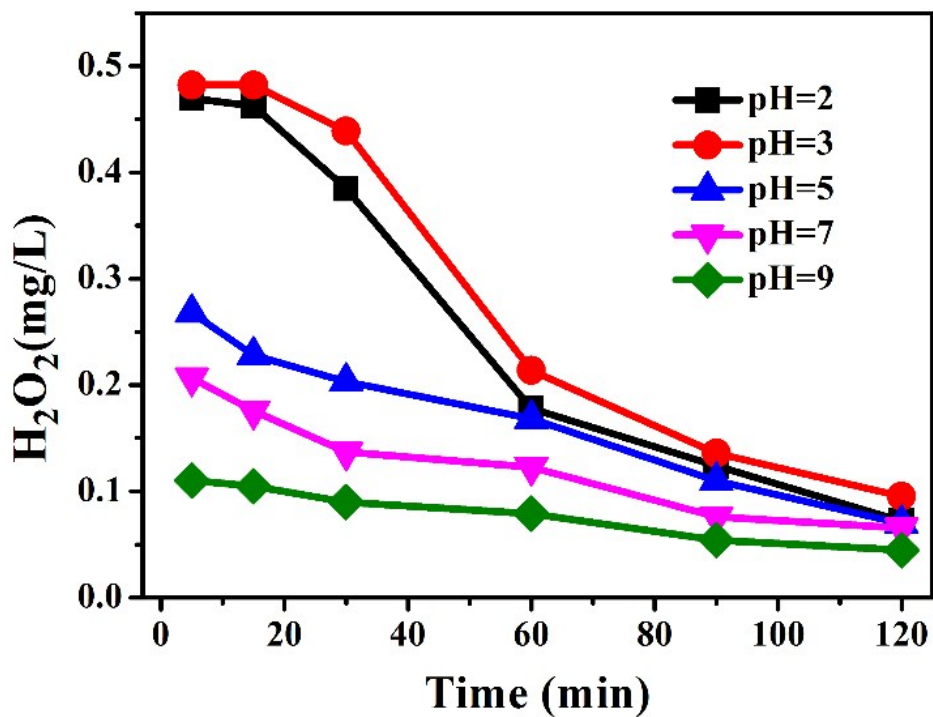


**Fig. S6** The concentration of electro-generated  $\text{H}_2\text{O}_2$  at different pH in PEF-like system with  $\text{WO}_3/\text{g-C}_3\text{N}_4$  (1:6).

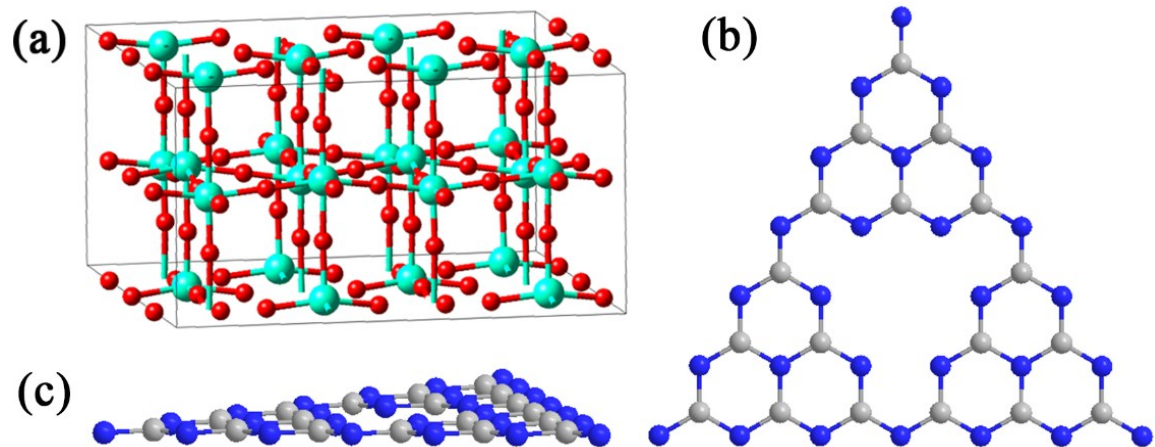


**Fig. S7** Crystal structures of monoclinic  $\text{WO}_3$  (a) and  $\text{g-C}_3\text{N}_4$  (b, c).

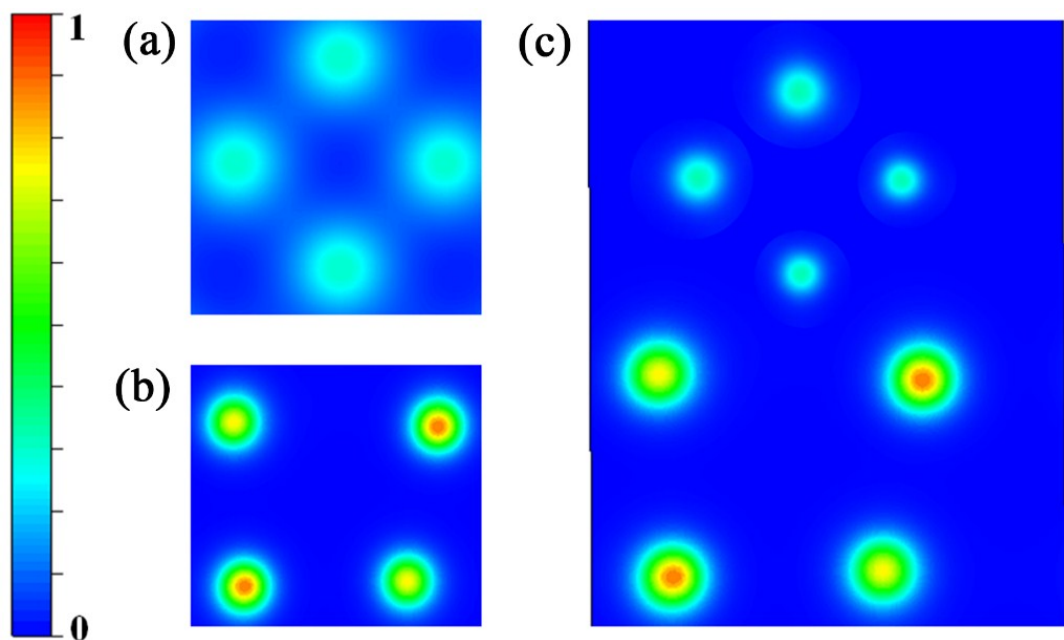


**Fig. S8** Electron density maps of  $\text{WO}_3$  (a),  $\text{g-C}_3\text{N}_4$  (b) and  $\text{WO}_3/\text{g-C}_3\text{N}_4$  model. Blue and red represented the most electro-poor and electro-rich regions, respectively.

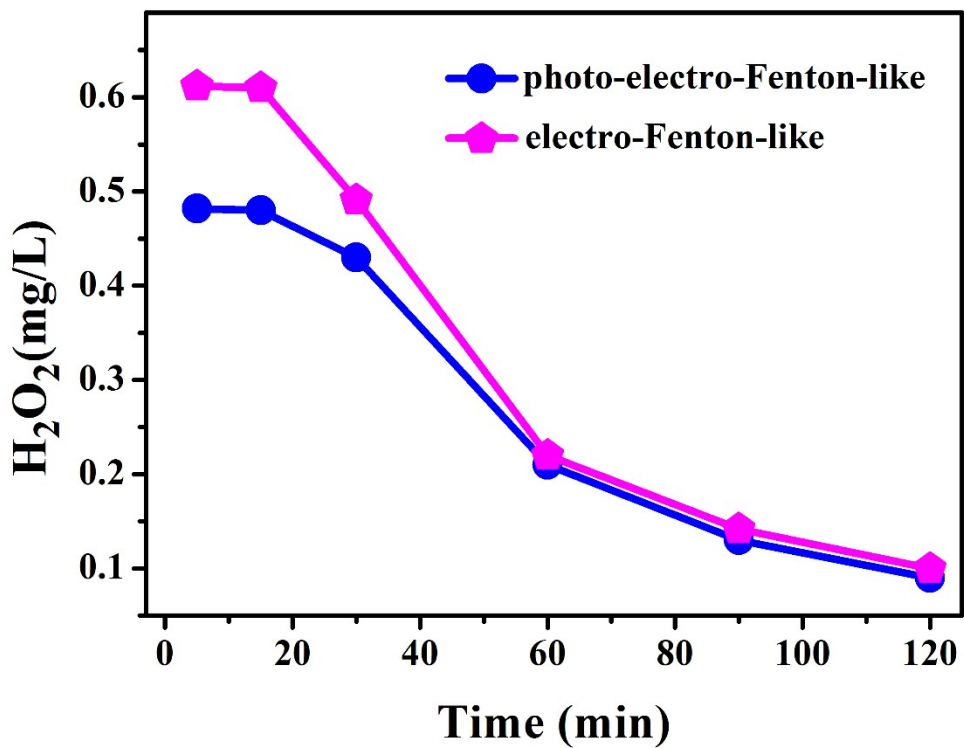


**Fig. S9** The concentration of electro-generated  $\text{H}_2\text{O}_2$  in PEF-like system and EF-like system with  $\text{WO}_3/\text{g-C}_3\text{N}_4$ (1:6).

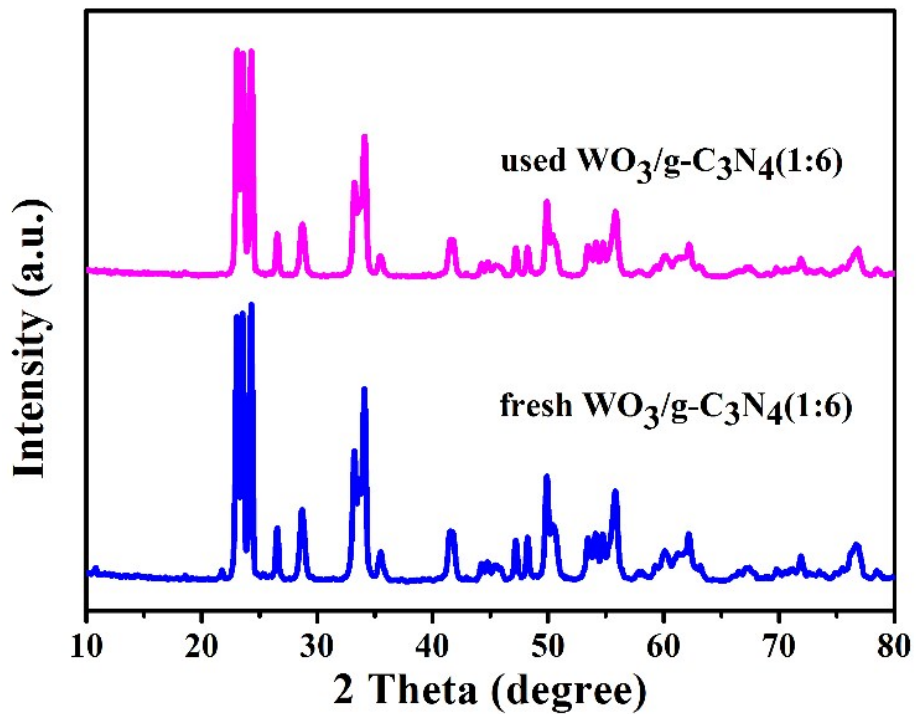


**Fig. S10** XRD patterns of fresh and used  $\text{WO}_3/\text{g-C}_3\text{N}_4$ (1:6) in PEF-like system.

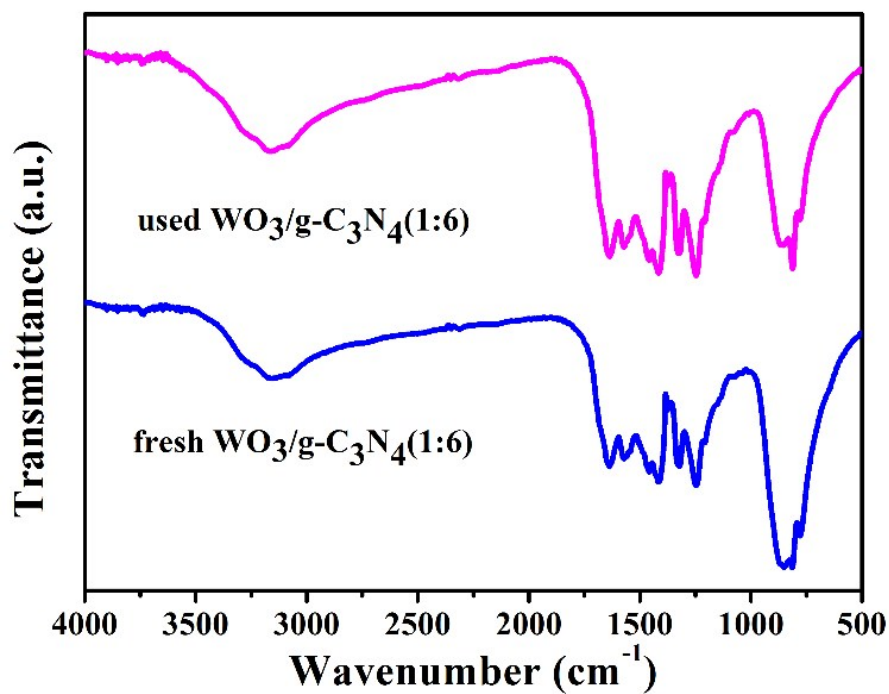


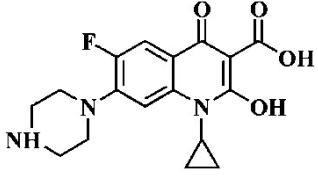
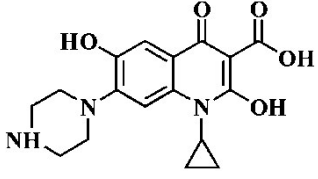
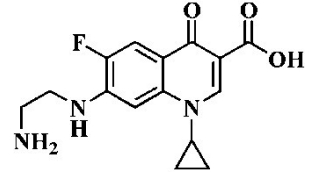
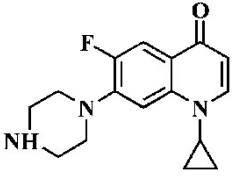
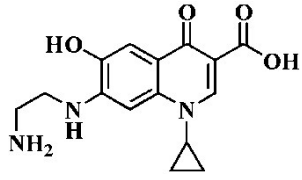
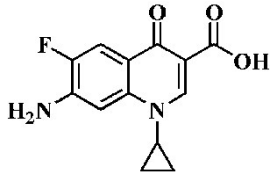
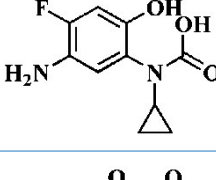
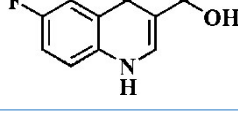
**Fig. S11** FT-IR spectrum of fresh and used WO<sub>3</sub>/g-C<sub>3</sub>N<sub>4</sub>(1:6) in PEF-like system.

**Table S1** Summary of the textural parameters of the samples.

Samples	Specific surface area (m <sup>2</sup> .g <sup>-1</sup> )	Pore volume (cm <sup>3</sup> .g <sup>-1</sup> )	Average pore size (nm)
g-C <sub>3</sub> N <sub>4</sub>	15.04	0.102	27.36
WO <sub>3</sub>	18.63	0.145	31.11
WO <sub>3</sub> /g-C <sub>3</sub> N <sub>4</sub> (1:6)	26.33	0.101	15.38

**Table S2** The intermediates of CIP degradation.

Compounds	Molecular formula	Structural formula	m/z
CIP	C <sub>17</sub> H <sub>18</sub> FN <sub>3</sub> O <sub>3</sub>	The chemical structure shows a 4-fluorophenyl ring attached to a piperazine ring, which is further attached to a 2,4-dioxo-2,3-dihydro-1H-pyridine-3-carboxylic acid ring. A cyclopropyl group is also present on the pyridine ring.	332

A	C <sub>16</sub> H <sub>18</sub> FN <sub>3</sub> O <sub>4</sub>		348
B	C <sub>17</sub> H <sub>19</sub> N <sub>3</sub> O <sub>4</sub>		330
C	C <sub>15</sub> H <sub>16</sub> FN <sub>3</sub> O <sub>3</sub>		306
D	C <sub>16</sub> H <sub>18</sub> FN <sub>3</sub> O		288
E	C <sub>15</sub> H <sub>17</sub> N <sub>3</sub> O <sub>4</sub>		304
F	C <sub>13</sub> H <sub>11</sub> FN <sub>2</sub> O <sub>3</sub>		263
G	C <sub>10</sub> H <sub>11</sub> FN <sub>2</sub> O <sub>3</sub>		227
H	C <sub>10</sub> H <sub>5</sub> FNO <sub>3</sub>		204